◆ Human Brain Mapping 35:4706–4717 (2014) ◆

Brain Networks Disconnection in Early Multiple Sclerosis Cognitive Deficits: An Anatomofunctional Study

Céline Louapre,[1,2,3,4] Vincent Perlbarg,[5,6] Daniel García-Lorenzo,[1,2,3,6] Marika Urbanski,[1,2,3,7] Habib Benali,[5,6] Rana Assouad,[4,6] Damien Galanaud,[1,2,3,4] Léorah Freeman,[1,2,3,4] Benedetta Bodini,[1,2,3] Caroline Papeix,[4,6] Ayman Tourbah,[8] Catherine Lubetzki,[1,2,3,4,6] Stéphane Lehéricy,[1,2,3,4] and Bruno Stankoff[1,2,3,4]*

[1]*Université Pierre et Marie Curie-Paris 6, Centre de Recherche de l'Institut du Cerveau et de la Moelle épinière, UMR-S975, Paris F-75013, France*
[2]*Inserm, U975, Paris F-75013, France*
[3]*CNRS, UMR 7225, Paris France*
[4]*AP-HP, Hôpital de la Salpêtrière, Hôpital Tenon, F-75020 Paris, France*
[5]*Inserm, UMR_S 678, Laboratoire d'Imagerie Fonctionnelle, Paris, France*
[6]*Institut des Neurosciences translationnelles de Paris (IHU-A-ICM), Paris, France*
[7]*Service de médecine et de réadaptation, Hôpital National de Saint-Maurice, France*
[8]*Université Champagne Ardennes, CHU de Reims, France*

Abstract: Severe cognitive impairment involving multiple cognitive domains can occur early during the course of multiple sclerosis (MS). We investigated resting state functional connectivity changes in large-scale brain networks and related structural damage underlying cognitive dysfunction in patients with early MS. Patients with relapsing MS (3–5 years disease duration) were prospectively assigned to

Additional Supporting Information may be found in the online version of this article.

Contract grant sponsors: ARSEP Foundation and JNLF; Contract grant number: ANR-10-IAIHU-06.

*Correspondence to: Bruno Stankoff, Université Pierre et Marie Curie-faculté de Médecine, service de neurologie, Hôpital Tenon, 4 rue de la Chine, 75020 Paris, France. E-mail: bruno.stankoff@tnn.aphp.fr

Celine Louapre has received lecture fees from Novartis. Rana Assouad report consulting fees from Biogen-Idec and Teva. Damien Galanaud reports consulting fees from Olea Médical (La Ciotat, France), Sanofi Aventis (Paris, France), and Biogen (Cambridge, MA). Caroline Papeix reports receiving consulting fees from Biogen Idec, Novartis, Merck Serono, Sanofi-Aventis, Teva-Pharma Bayer-schering, Genzyme, and Roche. Ayman Tourbah reports receiving consulting and lecture fees from Sanofi-Aventis-Genzyme, Teva-Pharma and research support from Biogen Idec, Novartis, Merck Serono Sanofi Aventis, participating in clinical trials for Biogen Idec, Novartis, Merck Serono, Bayer, and Roche. Catherine Lubetzki reports consulting fees from Roche, Novartis, Sanofi Aventis, and Teva Pharma, lecture fees from Merck-Serono, Biogen-Idec, Sanofi Aventis, and Teva, participating in clinical trials for Biogen Idec, Novartis, Merck Serono, Bayer-schering, Sanofi Aventis, Teva Pharma, Genzyme, and Roche. Bruno Stankoff reports receiving consulting and lecture fees from Biogen Idec, Novartis, Merck Serono, Sanofi-Aventis, Genzyme, Teva-Pharma, and Bayer and research support from Biogen Idec, Sanofi Aventis. Vincent Perlbarg, Daniel Garcia-Lorenzo, Marika Urbanski, Habib Benali, Leorah Freeman report no disclosure.

Stephane Lehéricy and Bruno Stankoff contributed equally to the work.

Received for publication 1 May 2013; Revised 22 February 2014; Accepted 25 February 2014.

DOI 10.1002/hbm.22505

Published online 31 March 2014 in Wiley Online Library (wileyonlinelibrary.com).

two groups based on a standardized neuropsychological evaluation: (1) cognitively impaired group (CI group, $n = 15$), with abnormal performances in at least 3 tests; (2) cognitively preserved group (CP group, $n = 20$) with normal performances in all tests. Patients and age-matched healthy controls underwent a multimodal 3T magnetic resonance imaging (MRI) including anatomical T1 and T2 images, diffusion imaging and resting state functional MRI. Structural MRI analysis revealed that CI patients had a higher white matter lesion load compared to CP and a more severe atrophy in gray matter regions highly connected to networks involved in cognition. Functional connectivity measured by integration was increased in CP patients versus controls in attentional networks (ATT), while integration was decreased in CI patients compared to CP both in the default mode network (DMN) and ATT. An anatomofunctional study within the DMN revealed that functional connectivity was mostly altered between the medial prefrontal cortex (MPFC) and the posterior cingulate cortex (PCC) in CI patients compared to CP and controls. In a multilinear regression model, functional correlation between MPFC and PCC was best predicted by PCC atrophy. Disconnection in the DMN and ATT networks may deprive the brain of compensatory mechanisms required to face widespread structural damage. *Hum Brain Mapp 35:4706–4717, 2014.*

Key words: multiple sclerosis; cognition; MRI; resting state; default mode network

INTRODUCTION

Multiple sclerosis (MS)-related cognitive disorders are often minor and circumscribed to restricted cognitive domains at the earliest stages (Amato et al., 2010a; Chiaravalloti and DeLuca, 2008; Feuillet et al., 2007; Reuter et al., 2011), but tend to extend to multiple domains with disease progression (Amato et al., 2010b; Reuter et al., 2011). However, severe cognitive disorders sometimes occur early in the relapsing phase of the disease, and subsequently deeply impact daily living for these young subjects.

The mechanisms responsible for cognitive impairment are probably many and not exclusive (Filippi et al., 2010). The macroscopic white matter (WM) lesion load is considered to be higher in patients with cognitive impairment compared to patients without cognitive disorder, but only partly explains the deficits (Rovaris et al., 2006). Diffuse microscopic WM abnormalities (Dineen et al., 2009; Fink et al., 2010; Roosendaal et al., 2009; Yu et al., 2012) together with gray matter (GM) pathology, including demyelinating cortical lesions (Calabrese et al., 2009), thalamic and cortical atrophy (Morgen et al., 2006) as well as inadequate cortical plasticity (Filippi et al., 2010; Rocca et al., 2010) also contribute to the cognitive deterioration. Functional connectivity within large-scale brain networks such as the default mode network (DMN) is considered an important factor associated with cognition and is thought to preserve efficient cognitive performances (Newton et al., 2011). Recent investigations of DMN connectivity by resting state functional magnetic resonance imaging (fMRI) in MS subjects have provided controversial results. Cognitive deficits have been associated either with a decrease (Bonavita et al., 2011; Rocca et al., 2010) or an increase (Hawellek et al., 2011) in DMN functional connectivity. Therefore, the implication of DMN functional connectivity changes on cognitive impairment remains elusive. The interpretation of many earlier studies in the field of MS-related cognitive disorders is obscured by the heterogeneity of patients studied in terms of disease course and duration as well as by the disparity in the definition of cognitive impairment.

To gain insight into the large scale brain networks connectivity changes underlying the severe cognitive deficit that may occur early in the disease course, we investigated here by multimodal MRI two groups of early relapsing remitting MS (RRMS) patients with the same disease duration, that were strongly contrasted for cognitive performances. Following brain network identification, we selected the one involved in cognition and assessed their functional connectivity changes. We therefore focused on the most affected network, the DMN, to perform an anatomofunctional study.

MATERIALS AND METHODS

Subjects and Evaluations

Approval of local ethics committee was obtained and all subjects gave written informed consent (clinicaltrials.gov NCT 01157728). RRMS patients aged 18–40, with disease duration between 3 and 5 years were prospectively included. Neurologists in charge of MS patients were asked to identify those who could fulfill inclusion criteria, either with presumed normal cognitive functioning, or with possible cognitive impairment. Identified subjects were then included in the study, and a standardized neuropsychological evaluation consisting in the seven following tests was performed (Dujardin et al., 2004): (1) Mattis dementia rating scale (MDRS; Hugonot-Diener et al., 2008; Schmidt et al., 1994), (2) PASAT-3 (Reuter et al., 2010), (3) trail making test (TMT; Godefroy et al., 2010), (4) verbal

fluency (literal and semantic stimulus; Cardebat et al., 1990), (5) digit span (Wheschler, 1981), (6) 10/36 spatial recall test (Boringa et al., 2001), and (7) Free and Cued Recall test (RL-RI 16 items; Van der Linden et al., 2004), a French validated version of the Grober and Buschke test. According to normative values previously validated in French subjects for each test, scores below −1.5 standard deviations (SDs) from the mean were considered as pathological (Ruet et al., 2013). In order to form highly contrasted groups for cognitive performance, patients were stratified as followed:

- Normal performance in all tests characterized cognitively preserved patients (CP MS).
- Pathological performance in at least 3 tests characterized cognitively impaired patients (CI MS).
- Patients displaying an intermediate cognitive profile (1 or 2 tests failed) were excluded (12 patients).

The stratification was established to fit with our working hypothesis, the identification of resting state changes underlying the occurrence of a severe cognitive impairment early in disease. This justified the choice of at least 3 tests impaired to identify such patients, as it was reported that the threshold of 3 tests failed allows to discriminate between patients with a severe cognitive impairment (at least 3 tests failed) from patients with a mild cognitive impairment (1 or 2 tests failed), and from patients without cognitive impairment (no failure; Calabrese et al., 2010).

We finally retained 20 CP MS, 15 CI MS patients and also recruited 20 aged-matched healthy volunteers (HVs).

Fatigue and depression were also investigated using the fatigue impact scale (FIS) and the Montgomery-Åsberg Depression Rating Scale, respectively.

MRI Scanning Protocol

MRI examination was performed using a 3T Siemens TRIO 32-channel TIM system, with body coil for transmission and 12-channel head coil for signal reception. Three-dimensional T1-weighted (3D-T1) magnetization prepared rapid acquisition gradient echo sagittal images [repetition time (TR)/echo time (TE): 2300/4.18 ms, flip angle: 9°, field of view (FOV): 256 mm × 256 mm, and voxel size 1 mm × 1 mm × 1 mm] were acquired for volumetric and registration procedures. For the measurement of T2 lesion load, the following sequences were acquired: Turbo spin echo dual-echo (proton density and T2; TR/TE1/TE2: 4100/14/69 ms, 40 axial slices, slice thickness: 3 mm, voxel size: 0.9 mm × 0.9 mm, and FOV: 230 mm × 230 mm), and T2 FLAIR (TR/TE: 8880/128 ms, TI: 2500 ms, 40 axial slices, slice thickness: 3 mm, voxel size: 0.9 mm × 0.9 mm, and FOV: 230 mm × 230 mm). For the measurement of T1-black-holes lesion load, we acquired a T1-spin echo sequence (TR/TE: 700/14 ms, 40 axial slices, slice thickness: 3 mm, voxel size: 0.9 mm × 0.9 mm, and FOV: 230 mm × 230 mm).

Resting-state fMRI acquisition included 200 volumes of echo planar images (TR/TE: 2100/25 ms, 36 axial slices, voxel size: 2 mm × 2 mm × 2 mm, and FOV: 192 mm × 192 mm). During this acquisition, subjects were asked to rest with eyes closed, not to fall asleep, and to think of nothing in particular. To analyze WM tracts, diffusion-weighted spin-echo echo-planar images were acquired (TR/TE:10s/86ms, flip angle; 90°, voxel size: 2 mm × 2 mm × 2 mm, 56 axial slices, and no gap) using 50 noncollinear diffusion gradients (b value of 1,000 s/mm^2) and one volume without diffusion weighting (b0 reference image).

Analysis of Structural Brain Pathology

WM lesion load and black holes segmentation

FLAIR and 3D-T1 were realigned on T2 sequences using SPM8 software (Wellcome Department of Cognitive Neurology, London, UK, http://www.fil.ion.ucl.ac.uk/spm/). Lesions were manually outlined on T2-weighted images, using the coregistered information of FLAIR and 3D-T1 images when boundaries of the lesions were not precise enough, especially around the ventricle. Lesion masks were registered on the 3D-T1 images using a 12-parameter affine transformation (FLIRT tool, part of FSL) and subsequently normalized on the MNI space using a nonlinear registration procedure (FNIRT tool, part of FSL). Normalized T2 lesion volume was calculated (fslstats, part of FSL). We applied the same procedure to segment black holes lesions on T1-spin echo sequences and calculate the normalized T1 black holes volume.

Localization of cortical atrophy

First, to avoid bias due to hypointense WM lesions that may be segmented as GM, we performed a step of lesion inpainting based on the T2 lesion mask registered to the 3D-T1 images as described previously (Chard et al., 2010). Voxel-based morphometry (VBM) data analysis was performed on 3D-T1 inpainted images using VBM8 toolbox, part of SPM8, and MATLAB version 2010a (The Mathworks, MA). This toolbox combines denoising (Manjon et al., 2010), tissue segmentation (Rajapakse et al., 1997), partial volume estimation (Tohka et al., 2004), and DARTEL normalization (Ashburner, 2007) in order to provide the GM, WM, and CSF normalized maps (Good et al., 2001). To improve the registration step, the DARTEL toolbox was used to create a group specific template that was aligned to the MNI space. Modulated normalized GM images were then smoothed with a 4-mm FWHM kernel.

GM volumes were calculated from the modulated normalized GM images, both for the total GM volume and for GM volume within specific clusters of interest identified by the VBM analysis.

Resting State fMRI Analysis

Functional images were corrected for slice timing, realigned to compensate for rigid movements and smoothed with a 3-mm FWHM kernel (SPM8). We automatically identified functional networks characterizing the full population by using the NetBrainWork toolbox (http://sites.google.com/site/netbrainwork) based on independent component analysis (ICA).

Thirty-five clusters were identified after initial ICA. We selected the networks with a good degree of representativity (the number of runs representing in the class), and a good degree of unicity (the number of runs representing by only one component). After this selection, we were able to identify the major networks reported in the literature: (i) involved in cognition: the default-mode network (DMN), the fronto-parietal attentional networks (ATT), the dorsal attentional network (dATT) and (ii) noncognitive: the sensory-motor network (MOT), the visual networks (medial and lateral visual network, identified as a single network in some subjects). Representativity of the dorsal attentional network was 0.52 whereas other networks had representativity above 0.8. Among these networks, we selected the one involved in cognition: DMN, left and right frontoparietal/attentional network, dorsal attentional (Majerus et al., 2012; Newton et al., 2011; Spreng et al., 2013). We compared these networks of interest for cognition to the motor network as a within-subject control, for the reason that our groups of patients were strongly contrasted for cognitive performance but were identical for motor performance, as they did not have any motor impairment. In contrast, the visual network was considered far from the hypothesis we wanted to test and was discarded.

Networks of interest for cognition were then selected to automatically identify regions of interest (ROIs) that were designed around the peaks of the map by using a region growing algorithm controlling the size (100 voxels) and the minimal distance (30 mm) between regions (coordinates in Supporting Information Table I). For subsequent functional connectivity analysis, functional time-series were corrected from physiological noise by using CORSICA (Perlbarg et al., 2007). Finally, we evaluated the degree of connectivity within each selected network by computing the functional integration (Marrelec et al., 2008). The functional integration is a measure originated from information theory (Watanabe, 1960), which captures the global level of statistical dependence of regional blood oxygen level-dependent time series within a brain system.

Functional and Structural Disconnection Within the DMN

The DMN, which showed the major functional disconnection in CI MS subjects, connects areas involved both in executive and frontal functions and in mnesic storage. To gain further insight in the structural abnormalities underlying this disconnection, we performed an anatomofunctional connectivity analysis within two distinct pathways belonging to the DMN: the anterior cingulum between medial prefrontal cortex (MPFC) and PCC (posterior cingulate cortex), and the posterior cingulum between PCC and PHG (parahippocampal gyrus) (coordinates in Supporting Information Table II). To quantify functional connectivity, we calculated pairwise correlations between PCC and MPFC and between PCC and PHG. In parallel, diffusion tensor imaging (DTI) maps were computed using Diffusion Toolbox, (FMRIB's Software Library, FSL) and subsequently normalised on FSL's fractional anisotropy (FA) template (FA_2_FMRIB58_1mm) using FNIRT. JHU WM tractography atlas was used to extract the anterior cingulum and the posterior cingulum for each subject. Finally, we computed the averaged FA, radial diffusivity (RD), and axial diffusivity (AD) along each tract. We decided to merge right and left anterior cingulum data because both sides connect MPFC and PCC due to their medial position (data from probabilistic tractography, not shown) and both sides are likely to reflect the anatomical connectivity underlying the functional correlation between MPFC and PCC.

In order to calculate WM lesion load and black holes volume within each tract, we registered the T2 and T1 lesion mask to the B0 volume for each patient using FLIRT tool from FSL, then warped it onto the JHU WM tractography template using the FNIRT transformation obtained previously. Fslmaths and fslstats, part of FSL, were used for the masking and volume calculation.

TABLE I. Demographic and clinical characteristics

	CP MS	CI MS	HV
Number of patients	20	15	20
Sex ratio (M/F)	8/12	1/14	10/10[a]
Age (years)	32.5 (5.0)	28.3 (6.7)	29.7 (5.5)
Education (years)	14.8 (3.1)	13.4 (2.6)	15.6 (2.4)
Disease duration (years)	4.5 (0.9)	4.6 (1.0)	–
EDSS score	1.0 (1.0)	3.0 (0.8)[b]	–
Pyramidal functional score	0.3 (0.6)	0.5 (0.7)	–
FIS score	53.8 (31.5)	89.4 (33.7)[c]	38.9 (28.6)

SD: standard deviation; CP MS: cognitively preserved MS patients; CI MS: cognitively impaired MS patients; HV: healthy volunteers.
Values are expressed as mean (SD).
[a]CI MS versus HV: $P < 0.05$.
[b]CI MS versus CP MS: $P < 5 \times 10^{-5}$.
[c]CI MS versus CP MS and HV: $P < 5 \times 10^{-4}$.

Statistical Analysis

Statistical group comparisons were performed using R software (http://r-project.org/, version 2.13). Gender repartition in the three groups (CI MS, CP MS, and HV)

TABLE II. Neuropsychological results

	CP MS	CI MS	HV	*P* value[a]
MDRS (/144)	142 (2)	137 (5)	142 (2)	$<5 \times 10^{-3}$
PASAT (/60)	51 (8)	30 (7)	50 (7)	$<5 \times 10^{-9}$
Digit span	11 (2)	5 (3)	10 (3)	$<5 \times 10^{-5}$
TMT A (s)	22 (5)	41 (16)	22 (8)	$< 5 \times 10^{-5}$
TMT B (s)	52 (13)	105 (29)	53 (23)	$<5 \times 10^{-6}$
SR10/36 (/36)	21 (5)	16 (4)	21 (4)	$<5 \times 10^{-3}$
SR-D 10/36 (/10)	8 (2)	6 (2)	9 (2)	0.02
Lexical fluency	24 (6)	17 (6)	24 (7)	$<5 \times 10^{-3}$
Semantic fluency	37 (9)	27 (10)	37 (9)	$<5 \times 10^{-3}$
RL-RI 16 items				
Immediate free recall/48	37 (6)	32 (6)	38 (4)	0.03
Immediate total recall/48	47 (2)	46 (3)	47 (1)	ns
Delayed free recall/16	14 (2)	12 (3)	14 (1)	0.02
Delayed total recall/16	15.8 (0.5)	15.6 (1.0)	15.8 (0.3)	ns

Results are expressed as means (SDs).
MDRS: Mattis dementia rating scale; PASAT: paced auditory serial addition test; TMT: trail making test; SR10/36: spatial recall test: SR-D 10/36: spatial recall test delayed.
[a]*P* value: CI MS versus CP MS and HV.

was analyzed using a χ^2 test. As a slight difference in the sex ratio between CI MS and HV patients was detected, we further assessed between-group differences in demographic, clinical, neuropsychological, and diffusion data (FA, RD, and AD), using an analysis of variance (ANOVA) controlled for sex. Fatigue and depression scales were also used as covariates for statistical comparisons as they may influence neuropsychological evaluation. Group comparisons were made between CI MS and CP MS groups, and then between each patient group and HV group. Post hoc comparisons were made using the Mann–Whitney *U*-test or the Student's *t*-test when data were normally distributed. *P* values <0.05 were considered statistically significant.

For the VBM analysis, group differences were inferred using voxel-level random-effects ANOVA with age, gender, and intracranial volume as covariates. A threshold at $P < 0.001$ with a correction for cluster extension was applied to the resultant statistical maps. Among the clusters identified with this threshold, we further outlined the clusters that were significant after family-wise error (FWE) correction at a threshold of $P < 0.05$.

For the resting-state functional connectivity analysis, group differences were inferred from the data using a fixed-effects group approach and a Bayesian group analysis with numerical sampling scheme (Marrelec et al., 2006). A probability of difference between groups >0.95 was considered significant.

A multimodal analysis was performed to assess the impact of different MRI measures on cognition by investigating the effect sizes (Cohen's *d*) between the two groups of patients.

A regression analysis with Spearman rank correlation and a stepwise multilinear regression model was used to assess whether functional connectivity within the DMN was associated with global and local WM and GM structural abnormalities in MS patients.

RESULTS

Demographical and Neuropsychological Characteristics of Subjects

Age, disease duration, and education level were not different between the 2 groups of patients (CI MS and CP MS). HV and CI MS patients slightly differed for gender ratio with more female in the CI group. EDSS score was low in all patients (mean score 1 and 3 in the CP MS and CI MS group, respectively), the difference being only due to the cerebral functional subscore (Table I).

When compared to CP MS group, the CI MS group had a strong defect in global cognitive performance (MDRS), sustained attention (digit span, PASAT), processing speed, working memory (PASAT), and executive functions (fluency, TMT; Table II). CI MS patients also had impaired free recall, but performance at the cued recall was unimpaired with no difference compared to both the CP MS and healthy controls groups, indicating preserved mnesic storage ability. Cognitive performances were identical between HVs and CP MS patients, and strongly decreased in CI MS compared to controls. Fatigue scores (FIS) were higher among CI MS patients compared to the two other groups.

WM Lesion Load

The total volume of T2 lesions was higher in CI MS patients (11.1 ± 13.6 cm^3) compared to CP MS patients (3.1 ± 3.7 cm^3). Black holes volume was also higher in CI

MS patients (0.51 ± 0.72 cm^3) compared to CP MS patients (0.08 ± 0.22 cm^3).

GM Atrophy

VBM analysis showed a greater decrease in GM volume in the CI MS group compared to CP MS in the frontal cortex (inferior, middle, and superior frontal gyrus), the posterior cingulate gyrus/cuneus, the supramarginal gyrus, the parahippocampal gyrus, the inferior and middle temporal gyrus, and basal ganglia (caudate and thalamus; Supporting Information Table III; Fig. 1). Several regions identified in this VBM analysis were highly connected with brain networks involved in cognition mainly the DMN (posterior cingulate gyrus, middle frontal gyrus, middle temporal gyrus, and parahippocampal gyrus) but also the attentional network (middle and inferior frontal and middle temporal gyri). Applying a very rigorous correction using FWE still led to the identification of atrophy in several regions of interest (left posterior cingulate gyrus, left inferior frontal gyrus, right thalamus, and bilateral caudate).

Resting State Network Analysis

Whole brain analysis by ICA allowed identification of several networks as previously described (Damoiseaux et al., 2006; Perlbarg and Marrelec, 2008). We analyzed selectively networks involved in cognition (Fig. 2A–C): the DMN, the frontoparietal attentional network (ATT), which was splited into right (ATT-R) and left (ATT-L) components, and the dATT. The motor (MOT) network was assessed as an internal control, as sensory-motor functions were identical between groups (Fig. 2D).

In the CI MS compared to CP MS group, total integration was significantly reduced in the DMN (−26%) and ATT networks (right: −38%; left: −26%) and in dorsal attentional network (−21%) but was not different in the MOT network (Fig. 2E). Although there were more females in the CI MS group than in the CP MS group, results were significant when corrected for gender.

In the CP MS group compared to HV, total integration was not different in the DMN and the MOT network, but

TABLE III. Effect size of MRI functional and structural metrics between the CP and CI MS groups

MRI metrics	Effect size (*d*)
Functional connectivity measures	
DMN integration	6.26
ATT-R integration	8.75
ATT-L integration	5.33
dATT integration	3.78
MPFC-PCC functional correlation	6.63
WM structural measures	
T2LV	−0.86
T1LV	−0.86
Ant cing FA	1.58
R post cing FA	1.17
L post cing FA	1.31
Ant cing AD	−0.39
R post cing AD	−0.71
L post cing AD	−0.63
Ant cing RD	−1.49
R post cing RD	−1.21
L post cing RD	−1.17
GM structural measures	
Normalized GM volume	1.22
PCC volume	1.44
LMFG volume	1.42

DMN: default mode network; ATT-R and ATT-L: right and left frontoparietal attentional networks; dATT: dorsal attention network; MPFC: medial prefrontal cortex; PCC: posterior cingulate cortex; ant cing: anterior cingulum; post cing: posterior cingulum; WM: white matter: GM; gray matter; T2LV: T2 lesion volume; T1LV; T1 lesion volume; LMFG: left middle frontal gyrus.

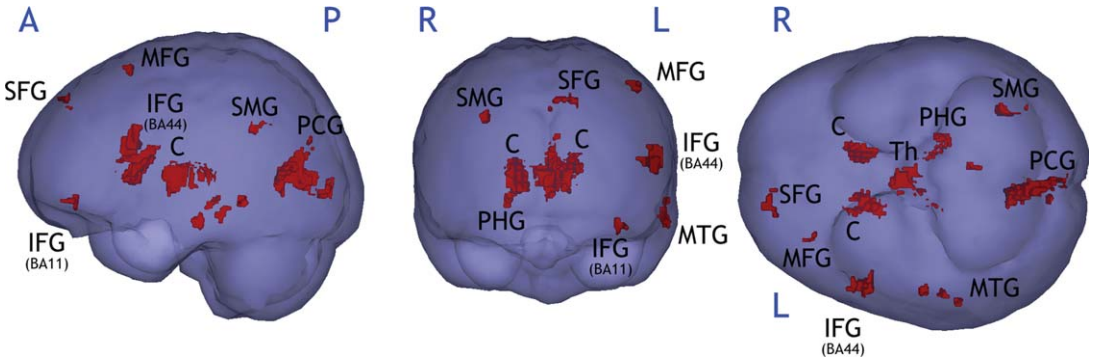

Figure 1.

Gray matter atrophy in CI MS patients compared to CP MS patients assessed by VBM ($P < 0.001$, $k = 216$ mm^2). SFG: superior frontal gyrus; MFG: medial frontal gyrus; IFG: inferior frontal gyrus; PCG: posterior cingulate gyrus; SMG: supramarginal gyrus; MTG: medial temporal gyrus; PHG: parahippocampal gyrus; Th: thalamus; C: caudate; BA: Brodmann area.

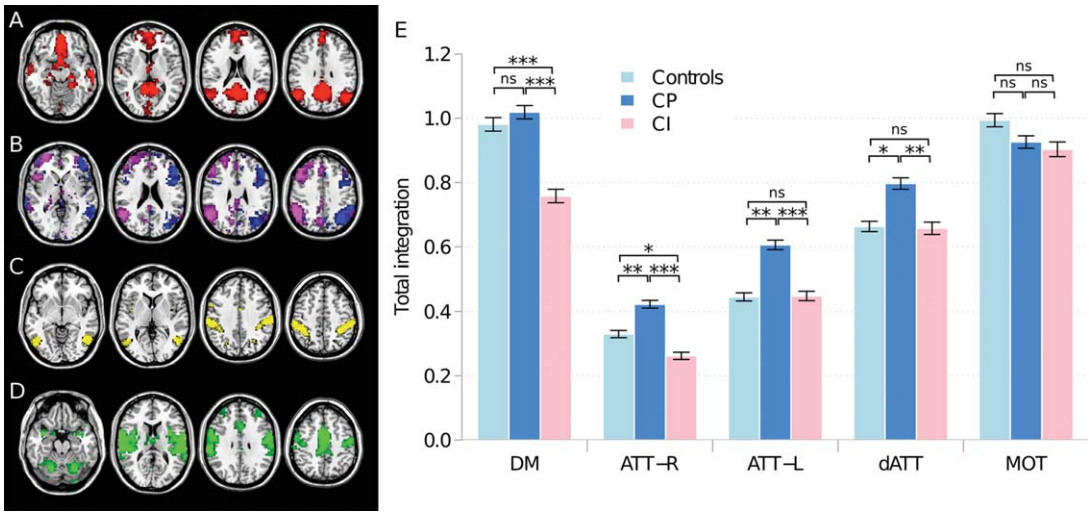

Figure 2.

(Left) Default mode, frontoparietal attentional, dorsal attentional and motor networks identified by independent component analysis. (**A**) Default mode network (DMN, red); (**B**) left (ATT-L, blue) and right (ATT-R, purple) frontoparietal attentional network; (**C**) dorsal attentional network (dATT, yellow); (**D**) motor network (MOT, green); and (right; **E**) total within-system integration in the DMN, ATT-R, ATT-L, dATT, and MOT; *: $P < 0.05$; **: $P < 5 \times 10^{-3}$; ***: $P < 5 \times 10^{-4}$; and ns: nonsignificant.

was significantly increased in both ATT networks (right ATT network: +22%; left ATT network: +26%) and in dorsal attentional network (+20%).

In the CI MS group compared to HV, total integration was significantly reduced in the DMN (−22%) and in the right ATT network (−14%), but it was not different in the left ATT network and in the dorsal attentional network (Fig. 2E).

Functional and Structural Measures Within the DMN: A Dissociation Between Attentional and Mnesic Pathways

As the preservation of mnesic storage contrasted with alteration of other cognitive functions in the CI MS group, we analyzed separately in the DMN that was the most disconnected network, (1) the ventral DMN component, which comprises the PCC and PHG and (2) the dorsal DMN component, which comprises MPFC and PCC. The fibre tract connecting these regions is mainly the cingulum (Greicius et al., 2009; van den Heuvel et al., 2009), divided in two parts: the anterior cingulum, connecting the MPFC to the PCC and involved in attention and frontal performance (Charlton et al., 2010; Schermuly et al., 2010), and the posterior cingulum, connecting the PCC to the PHG (Fig. 3A) and involved in mnesic storage itself (Charlton et al., 2010; Sasson et al., 2012).

Comparison between CI MS and CP MS patients

Functional correlation measures at the resting state were strongly reduced in CI MS between regions connected by the anterior cingulum (MPFC and PCC: −45%), but not between the regions connected by the posterior cingulum (PCC and PHG; Fig. 3B). By contrast, a significant decrease in mean FA in CI MS was found in both the anterior cingulum (16%) and the posterior cingulum (12% in the left, 11% in the right; Fig. 3C). RD was increased in CI MS both in anterior and posterior cingulum (+15% and +12%, respectively, Fig. 3D), whereas there was no difference in AD (Fig. 3E).

Regional macroscopic T2 lesion load was quantified in each of these tracts, and no difference between CI MS (anterior cingulum: 6 ± 16 mm^3 and posterior cingulum: 4 ± 12 mm^3) and CP MS patients (anterior cingulum: 4 ± 14 mm^3 and posterior cingulum: 0 mm^3) was found. The presence of T2 lesions within anterior and posterior cingulum did not impact on the measurement of FA and diffusivity as removing the T2 lesions from the analysis of these tracts did not modify our results. When total lesion load was considered, we found no correlation with FA in both posterior cingulum but a negative correlation was found between total lesion load and FA in the anterior cingulum ($r = -0.57$; $P = 0.0022$). No black hole lesions co-localized with the cingulum except in two CI MS patients and they impacted none of the DTI metrics.

Comparison between HV and CP MS patients

There was no difference in resting state correlation and diffusivity parameters for these regions, except for a difference in the RD within the left posterior cingulum (increase of 5% in CP MS patients compared to controls).

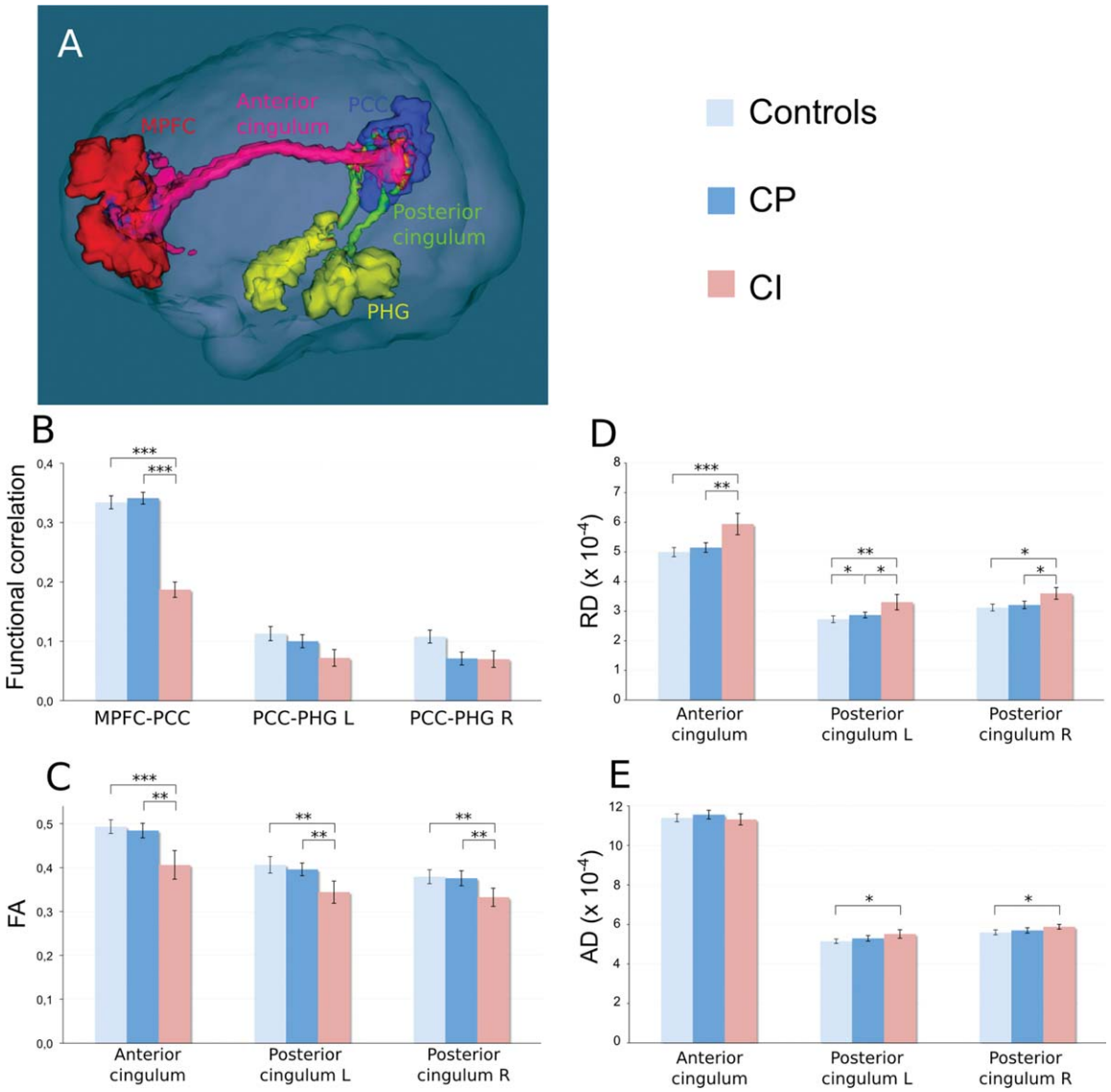

Figure 3.

Structural and functional measures within the default mode network. (**A**) 3D view of the three regions of interest in the DMN together with the bundles identified by tractography in a patient with MS. Red: medial prefrontal cortex (MPFC); blue: posterior cingulate/precuneus (PCC): yellow: parahippocampal gyrus (PHG); pink: anterior cingulum; and green: posterior cingulum. (**B**) Functional correlation between MPFC and PCC, PCC and left PHG, PCC and right PHG. (**C–E**) Mean FA, radial diffusivity (RD) and axial diffusivity (AD), respectively, within the anterior cingulum, the left posterior cingulum and the right posterior cingulum; *: $P < 0.05$; **: $P < 5 \times 10^{-3}$; ***: $P < 5 \times 10^{-4}$; and all other group differences were not statistically significant.

Comparison between HV and CI MS patients

We found significant differences between HV and CI MS patients for the same parameters than between CP MS and CI MS patients, with the addition of an increase in AD within the posterior cingulum (+5% in the right posterior cingulum and +6% in the left posterior cingulum in CI MS patients compared to HV; Fig. 3E).

Multimodal Analysis of Functional and Structural Data and Their Impact on Cognition

An effect size analysis was conducted between CP and CI MS groups for the most relevant MRI metrics (Table III). Resting state functional connectivity measures such as the ATT-R and DMN integration, as well as the MPFC-

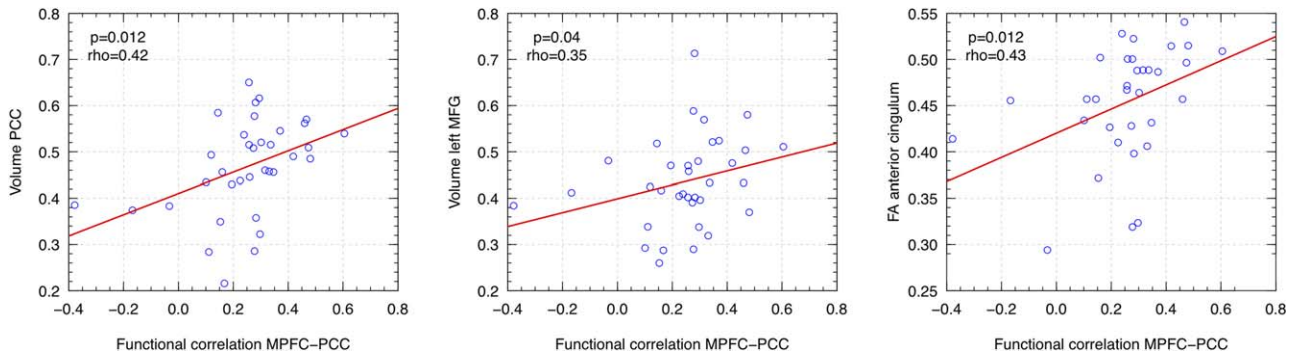

Figure 4.

Spearman rank correlation between functional connectivity within the DMN and structural imaging parameters. MPFC: medial prefrontal cortex; PCC: posterior cingulate cortex; MFG: middle frontal gyrus. [Color figure can be viewed in the online issue, which is available at wileyonlinelibrary.com.]

PCC functional correlation had the highest effect size (Cohen's *d* score 8.75, 6.26, and 6.63, respectively). Among structural data, anterior cingulum FA and PCC volume had a similar effect size (Cohen's *d* score 1.58 and 1.44, respectively).

To investigate the relationship between functional and structural abnormalities within the DMN, we performed a linear regression analysis between the MPFC-PCC resting state functional correlation and the most relevant structural imaging measures: (i) for GM volumes, total GM as well as left middle frontal gyrus (LMFG) and PCC (the two most significant GM clusters in the VBM analysis) and (ii) for WM integrity, DTI metrics (FA, AD, and RD) in the anterior and posterior cingulum, total T1 and T2 lesion volume, T1 and T2 lesion volume within the cingulum. MPFC-PCC functional connectivity showed a positive correlation with PCC volume, LMFG volume, and FA of the anterior cingulum only (Fig. 4). We subsequently performed a stepwise regression model including all the above structural variables to predict the functional connectivity between MPFC and PCC. Significant prediction was only obtained with one variable, which was the PCC volume ($P = 0.012$, $R^2 = 0.1605$, F-statistic = 7.116).

DISCUSSION

Our findings strongly suggest that modifications in functional connectivity identified using resting state fMRI are key players in the occurrence of the severe cognitive dysfunction observed in the CI MS group as: (i) preserved or enhanced connectivity within the DMN and both attentional networks was associated with preserved cognitive performances in the CP MS group, (ii) preserved connectivity in other specific networks (involved in motor function and memory) was also associated with normal related clinical function, and (iii) reduced connectivity within the DMN and to a lesser extent, attentional networks, was associated with cognitive impairment. The matching between the two MS groups for age, noncognitive EDSS scores, disease duration, and education level, allowed a selective investigation of cognition impairment-related mechanisms, focusing on large-scale brain networks connectivity. The dichotomy between the two patients group was based on an extensive neuropsychological battery in order to investigate broad cognitive domains such as attention, processing speed, verbal and visuospatial learning and memory. We acknowledge that interpretation of neuropsychological testing could be limited by the lack of specificity and practice effects previously reported for the PASAT (Polman and Rudick, 2010). However, defining cognitive impairment as the failure of at least three tests allowed to minimize this bias and to accurately define subjects with a severe and significant cognitive deficit. Although there was a difference in the gender ratio between patients and HVs, statistical comparisons remained significant when controlled for gender. The correction for gender was required here as gender has been reported to influence structural and functional parameters in MS. A more severe deep GM atrophy was found in male compared to female patients (Schoonheim et al., 2012), the male having a more severe cognitive impairment than female in that study. As well, a weaker functional connectivity in male compared to female patients was reported within the DMN (Koenig et al., 2013).

Few studies to date have investigated the relationship between resting state connectivity and cognitive status of MS patients, with apparent conflicting results. Following the clinically isolated syndrome (CIS), an increase in the connectivity within the DMN was identified with a subsequent return to normal level during the RR phase (Roosendaal et al., 2010). Whether such an early increase in connectivity could be linked to cognition or could reflect a more general brain adaptive mechanism remains to date unsolved. Later on during MS course, connectivity was found to be reduced in the DMN together with the

accumulation of cognitive deficits in RRMS (Bonavita et al., 2011) as well as in a cohort of progressive MS subjects with various levels of cognitive deficits (Rocca et al., 2010), which was in accordance with our results. This contrasted with a recent report showing that increased connectivity in the DMN during the very early RR phase was associated with worse cognitive performances (Hawellek et al., 2011). The slight methodological differences between the reported studies could provide some explanation for these discrepancies. In particular while all studies used ICA derived methods, allowing the identification of temporally coherent networks that are usually consistent among subjects (Calhoun et al., 2008), different software were then employed for network connectivity quantification (Bonavita et al., 2011; Cruz-Gomez et al., 2014; Hawellek et al., 2011; Rocca et al., 2010). Studies differed also between a totally data-driven analysis (Hawellek et al., 2011) and a hypothesis driven analysis of networks implied in cognitive processes. Here, we used a two-step method consisting in an automatic definition of regions of interest based on ICA followed by the calculation of functional integration within the networks selected on physiopathological hypothesis. To go further, we proposed to jointly study functional and structural connectivity from the same regions. This allows to directly investigate the functional connectivity disorder and structural damage in the same bundles, as done here for the cingulum.

An alternative explanation for these discrepancies could be related to the different levels of compensatory mechanisms at distinct stages of the disease. Following CIS, an increase in DMN connectivity could be interpreted as a compensatory mechanism aimed at preventing the onset of cognitive deterioration. This would be in agreement with the study performed in RR patients (Hawellek et al., 2011), showing increased DMN connectivity associated with cognitive symptoms, as most patients in this study only displayed minor cognitive abnormalities (with failure at one or few tests and restricted cognitive domains involved). Therefore, DMN connectivity may be part of the compensatory mechanisms used by the brain to maintain global cognitive efficiency against structural WM injury, which supports the described influence of DMN on the cognitive reserve of MS patients (Sumowski et al., 2010).

Although previous studies have suggested a higher WM lesion load among patients with cognitive disorder (Rovaris et al., 2006), WM lesions only partly explained the cognitive symptoms and the relationship tended to disappear with disease progression (Kincses et al., 2011; Reuter et al., 2011). Accordingly, although we found a higher global lesion load in the CI MS group, the regional lesion load within cingulum did not differ between groups, whereas the strongest disconnection was found between MPFC and PCC, suggesting that the decrease in connectivity within the DMN was not a direct consequence of regional WM lesions. We further analyzed WM structural changes using DTI in anterior and posterior cingulum. A limitation of the study was that we used a single b0 to estimate the diffusion tensor, which could have reduced the sensitivity of these measures to detect changes in MS patients (Jones et al., 1999). However in CI MS patients, we found significant diffusivity abnormalities in both the anterior and posterior cingulum that contrasted with reduced functional connectivity within the anterior cingulum only. Therefore, the normal appearing WM (NAWM) pathology did not strictly parallel the level of disconnection within networks in our study.

As neither regional macroscopic lesions nor regional NAWM damage fully explained resting state connectivity changes, the functional disconnection in associative networks could be related to GM pathology, which has already been proposed to act on cognitive dysfunction (Amato et al., 2007; Calabrese et al., 2011; Morgen et al., 2006). In this respect, we showed that, in the CI MS group, cortical regions with pronounced atrophy were characterized by their multiple connections with associative networks. This was the case for the frontal gyri and the posterior cingulate gyrus, which are part of the DMN. In these regions, GM volume but also FA in the anterior cingulum significantly correlated with the functional connectivity between cortical regions of the DMN connected by the anterior cingulum (MPFC and PCC). However in the multilinear regression model including both measures of tissue integrity in the WM and GM compartment, the functional connectivity between MPFC and PCC was only predicted by the volume of PCC. Together with cortical pathology, the thalamic atrophy identified in CI MS subjects could be part of the triggering mechanisms, as DMN disconnection was described as a possible consequence of an MS thalamic lesion (Jones et al., 2011). Finally such a disconnection may deprive the brain of a crucial adaptive compensatory mechanism required to maintain cognitive efficiency.

In conclusion, we have characterized the functional connectivity changes in cognitive brain networks that underlie the occurrence of a severe cognitive impairment at an early stage of MS. The main abnormalities were a decrease in DMN connectivity, and to a lesser extent a decrease (or lack of increase) in frontoparietal and dorsal attentional networks. Overall, functional connectivity measures were the imaging parameters that had the highest effect size to discriminate CP and CI MS patients compared to structural MRI metrics.

These connectivity changes were not fully explained by structural WM pathology, and regional cortical atrophy in areas connected with these networks is thought to play a triggering role. In the future, evaluation of the resting state networks connectivity could open new ways to monitor disease progression and evaluate cognitive rehabilitation efficacy. Exploring connectivity changes in additional functional networks that have recently raised interest in cognitive domains such as the executive control network and the salience network would also be of potential interest.

ACKNOWLEDGMENTS

We thank the Centre d'Investigation Clinique team from ICM—Hôpital Pitié Salpêtrière and Jean-Christophe Corvol for the protocol organization, the imaging team of the CENIR, Romain Valabrègue, Eric Bardinet, Eric Bertasi for technical support, Sean Freeman for careful reading the manuscript, Anne-Claire Viret (Fondation Ophtalmologique Rothschild, Paris) and Jean Pelletier (CHU la Timone, Marseille, France), for fruitful discussions.

REFERENCES

Amato MP, Portaccio E, Goretti B, Zipoli V, Battaglini M, Bartolozzi ML, Stromillo ML, Guidi L, Siracusa G, Sorbi S, Federico A, De Stefano N (2007): Association of neocortical volume changes with cognitive deterioration in relapsing-remitting multiple sclerosis. Arch Neurol 64:1157–1161.

Amato MP, Portaccio E, Goretti B, Zipoli V, Hakiki B, Giannini M, Pasto L, Razzolini L (2010a): Cognitive impairment in early stages of multiple sclerosis. Neurol Sci 31:S211–S214.

Amato MP, Portaccio E, Goretti B, Zipoli V, Iudice A, Della Pina D, Malentacchi G, Sabatini S, Annunziata P, Falcini M, Mazzoni M, Mortilla M, Fonda C, De Stefano N (2010b): Relevance of cognitive deterioration in early relapsing-remitting MS: A 3-year follow-up study. Mult Scler 16:1474–1482.

Ashburner J (2007): A fast diffeomorphic image registration algorithm. Neuroimage 38:95–113.

Bonavita S, Gallo A, Sacco R, Corte MD, Bisecco A, Docimo R, Lavorgna L, Corbo D, Costanzo AD, Tortora F, Cirillo M, Esposito F, Tedeschi G (2011): Distributed changes in default-mode resting-state connectivity in multiple sclerosis. Mult Scler 17:411–422.

Boringa JB, Lazeron RH, Reuling IE, Ader HJ, Pfennings L, Lindeboom J, de Sonneville LM, Kalkers NF, Polman CH (2001): The brief repeatable battery of neuropsychological tests: Normative values allow application in multiple sclerosis clinical practice. Mult Scler 7:263–267.

Calabrese M, Agosta F, Rinaldi F, Mattisi I, Grossi P, Favaretto A, Atzori M, Bernardi V, Barachino L, Rinaldi L, Perini P, Gallo P, Filippi M (2009): Cortical lesions and atrophy associated with cognitive impairment in relapsing-remitting multiple sclerosis. Arch Neurol 66:1144–1150.

Calabrese M, Rinaldi F, Mattisi I, Bernardi V, Favaretto A, Perini P, Gallo P (2011): The predictive value of gray matter atrophy in clinically isolated syndromes. Neurology 77:257–263.

Calabrese M, Rinaldi F, Mattisi I, Grossi P, Favaretto A, Atzori M, Bernardi V, Barachino L, Romualdi C, Rinaldi L, Perini P, Gallo P (2010): Widespread cortical thinning characterizes patients with MS with mild cognitive impairment. Neurology 74:321–328.

Calhoun VD, Kiehl KA, Pearlson GD (2008): Modulation of temporally coherent brain networks estimated using ICA at rest and during cognitive tasks. Hum Brain Mapp 29:828–38.

Cardebat D, Doyon B, Puel M, Goulet P, Joanette Y (1990): Formal and semantic lexical evocation in normal subjects. Performance and dynamics of production as a function of sex, age and educational level [in French]. Acta Neurol Belg 90: 207–217.

Chard DT, Jackson JS, Miller DH, Wheeler-Kingshott CA (2010): Reducing the impact of white matter lesions on automated measures of brain gray and white matter volumes. J Magn Reson Imaging 32:223–228.

Charlton RA, Barrick TR, Lawes IN, Markus HS, Morris RG (2010): White matter pathways associated with working memory in normal aging. Cortex 46:474–489.

Chiaravalloti ND, DeLuca J (2008): Cognitive impairment in multiple sclerosis. Lancet Neurol 7:1139–1151.

Cruz-Gomez AJ, Ventura-Campos N, Belenguer A, Avila C, Forn C (2014): The link between resting-state functional connectivity and cognition in MS patients. Mult Scler 20:338–348.

Damoiseaux JS, Rombouts SA, Barkhof F, Scheltens P, Stam CJ, Smith SM, Beckmann CF (2006): Consistent resting-state networks across healthy subjects. Proc Natl Acad Sci USA 103: 13848–13853.

Dineen RA, Vilisaar J, Hlinka J, Bradshaw CM, Morgan PS, Constantinescu CS, Auer DP (2009): Disconnection as a mechanism for cognitive dysfunction in multiple sclerosis. Brain 132: 239–249.

Dujardin K, Sockeel P, Cabaret M, De Seze J, Vermersch P (2004): BCcogSEP: A French test battery evaluating cognitive functions in multiple sclerosis [in French]. Rev Neurol (Paris) 160:51–62.

Feuillet L, Reuter F, Audoin B, Malikova I, Barrau K, Cherif AA, Pelletier J (2007): Early cognitive impairment in patients with clinically isolated syndrome suggestive of multiple sclerosis. Mult Scler 13:124–127.

Filippi M, Rocca MA, Benedict RH, DeLuca J, Geurts JJ, Rombouts SA, Ron M, Comi G (2010): The contribution of MRI in assessing cognitive impairment in multiple sclerosis. Neurology 75: 2121–2128.

Fink F, Eling P, Rischkau E, Beyer N, Tomandl B, Klein J, Hildebrandt H (2010): The association between California Verbal Learning Test performance and fibre impairment in multiple sclerosis: Evidence from diffusion tensor imaging. Mult Scler 16:332–341.

Godefroy O, Azouvi P, Robert P, Roussel M, LeGall D, Meulemans T (2010): Dysexecutive syndrome: Diagnostic criteria and validation study. Ann Neurol 68:855–864.

Good CD, Johnsrude IS, Ashburner J, Henson RN, Friston KJ, Frackowiak RS (2001): A voxel-based morphometric study of ageing in 465 normal adult human brains. Neuroimage 14:21–36.

Greicius MD, Supekar K, Menon V, Dougherty RF (2009): Resting-state functional connectivity reflects structural connectivity in the default mode network. Cereb Cortex 19:72–78.

Hawellek DJ, Hipp JF, Lewis CM, Corbetta M, Engel AK (2011): Increased functional connectivity indicates the severity of cognitive impairment in multiple sclerosis. Proc Natl Acad Sci USA 108:19066–19071.

Hugonot-Diener L, Barbeau E, Michel B-F, Thomas-Antérion C, Robert, P (2008): GREMOIRE: Tests et échelles de la maladie d'Alzheimer et des syndromes apparentés. Marseille. Solal.

Jones DK, Horsfield MA, Simmons A (1999): Optimal strategies for measuring diffusion in anisotropic systems by magnetic resonance imaging. Magn Reson Med 42:515–525.

Jones DT, Mateen FJ, Lucchinetti CF, Jack CR Jr, Welker KM (2011): Default mode network disruption secondary to a lesion in the anterior thalamus. Arch Neurol 68:242–247.

Kincses ZT, Ropele S, Jenkinson M, Khalil M, Petrovic K, Loitfelder M, Langkammer C, Aspeck E, Wallner-Blazek M, Fuchs S, Jehna M, Schmidt R, Vecsei L, Fazekas F, Enzinger C (2011): Lesion probability mapping to explain clinical deficits

and cognitive performance in multiple sclerosis. Mult Scler 17: 681–689.

Koenig KA, Lowe MJ, Lin J, Sakaie KE, Stone L, Bermel RA, Beall EB, Rao SM, Trapp BD, Phillips MD (2013): Sex differences in resting-state functional connectivity in multiple sclerosis. AJNR Am J Neuroradiol 34:2304–2311.

Majerus S, Attout L, D'Argembeau A, Degueldre C, Fias W, Maquet P, Martinez Perez T, Stawarczyk D, Salmon E, Van der Linden M, Phillips C, Balteau E (2012): Attention supports verbal short-term memory via competition between dorsal and ventral attention networks. Cereb Cortex 22:1086–1097.

Manjon JV, Coupe P, Marti-Bonmati L, Collins DL, Robles M (2010): Adaptive non-local means denoising of MR images with spatially varying noise levels. J Magn Reson Imaging 31: 192–203.

Marrelec G, Bellec P, Krainik A, Duffau H, Pelegrini-Issac M, Lehericy S, Benali H, Doyon J (2008): Regions, systems, and the brain: Hierarchical measures of functional integration in fMRI. Med Image Anal 12:484–496.

Marrelec G, Krainik A, Duffau H, Pelegrini-Issac M, Lehericy S, Doyon J, Benali H (2006): Partial correlation for functional brain interactivity investigation in functional MRI. Neuroimage 32:228–237.

Morgen K, Sammer G, Courtney SM, Wolters T, Melchior H, Blecker CR, Oschmann P, Kaps M, Vaitl D (2006): Evidence for a direct association between cortical atrophy and cognitive impairment in relapsing-remitting MS. Neuroimage 30:891–898.

Newton AT, Morgan VL, Rogers BP, Gore JC (2011): Modulation of steady state functional connectivity in the default mode and working memory networks by cognitive load. Hum Brain Mapp 32:1649–1659.

Perlbarg V, Bellec P, Anton JL, Pelegrini-Issac M, Doyon J, Benali H (2007): CORSICA: Correction of structured noise in fMRI by automatic identification of ICA components. Magn Reson Imaging 25:35–46.

Perlbarg V, Marrelec G (2008): Contribution of exploratory methods to the investigation of extended large-scale brain networks in functional MRI: Methodologies, results, and challenges. Int J Biomed Imaging 2008:218519.

Polman CH, Rudick RA (2010): The multiple sclerosis functional composite: A clinically meaningful measure of disability. Neurology 74 Suppl 3:S8–15.

Rajapakse JC, Giedd JN, Rapoport JL (1997): Statistical approach to segmentation of single-channel cerebral MR images. IEEE Trans Med Imaging 16:176–186.

Reuter F, Zaaraoui W, Crespy L, Faivre A, Rico A, Malikova I, Soulier E, Viout P, Ranjeva JP, Pelletier J, Audoin B (2011): Frequency of cognitive impairment dramatically increases during the first 5 years of multiple sclerosis. J Neurol Neurosurg Psychiatry 82:1157–1159.

Reuter M, Rosas HD, Fischl B (2010): Highly accurate inverse consistent registration: A robust approach. Neuroimage 53:1181–1196.

Rocca MA, Valsasina P, Absinta M, Riccitelli G, Rodegher ME, Misci P, Rossi P, Falini A, Comi G, Filippi M (2010): Default-mode network dysfunction and cognitive impairment in progressive MS. Neurology 74:1252–1259.

Roosendaal SD, Geurts JJ, Vrenken H, Hulst HE, Cover KS, Castelijns JA, Pouwels PJ, Barkhof F (2009): Regional DTI differences in multiple sclerosis patients. Neuroimage 44:1397–1403.

Roosendaal SD, Schoonheim MM, Hulst HE, Sanz-Arigita EJ, Smith SM, Geurts JJ, Barkhof F (2010): Resting state networks change in clinically isolated syndrome. Brain 133:1612–1621.

Rovaris M, Comi G, Filippi M (2006): MRI markers of destructive pathology in multiple sclerosis-related cognitive dysfunction. J Neurol Sci 245:111–116.

Ruet A, Deloire M, Hamel D, Ouallet JC, Petry K, Brochet B (2013): Cognitive impairment, health-related quality of life and vocational status at early stages of multiple sclerosis: A 7-year longitudinal study. J Neurol 260:776–784.

Sasson E, Doniger GM, Pasternak O, Tarrasch R, Assaf Y (2012): Structural correlates of cognitive domains in normal aging with diffusion tensor imaging. Brain Struct Funct 217:503–515.

Schermuly I, Fellgiebel A, Wagner S, Yakushev I, Stoeter P, Schmitt R, Knickenberg RJ, Bleichner F, Beutel ME (2010): Association between cingulum bundle structure and cognitive performance: An observational study in major depression. Eur Psychiatry 25:355–360.

Schmidt R, Freidl W, Fazekas F, Reinhart B, Grieshofer P, Koch M, Eber B, Schumacher M, Polmin K, Lechner H (1994): The Mattis Dementia Rating Scale: Normative data from 1,001 healthy volunteers. Neurology 44:964–966.

Schoonheim MM, Popescu V, Rueda Lopes FC, Wiebenga OT, Vrenken H, Douw L, Polman CH, Geurts JJ, Barkhof F (2012): Subcortical atrophy and cognition: Sex effects in multiple sclerosis. Neurology 79:1754–1761.

Spreng RN, Sepulcre J, Turner GR, Stevens WD, Schacter DL (2013): Intrinsic architecture underlying the relations among the default, dorsal attention, and frontoparietal control networks of the human brain. J Cogn Neurosci 25:74–86.

Sumowski JF, Wylie GR, Deluca J, Chiaravalloti N (2010): Intellectual enrichment is linked to cerebral efficiency in multiple sclerosis: Functional magnetic resonance imaging evidence for cognitive reserve. Brain 133:362–374.

Tohka J, Zijdenbos A, Evans A (2004): Fast and robust parameter estimation for statistical partial volume models in brain MRI. Neuroimage 23:84–97.

van den Heuvel MP, Mandl RC, Kahn RS, Hulshoff Pol HE (2009): Functionally linked resting-state networks reflect the underlying structural connectivity architecture of the human brain. Hum Brain Mapp 30:3127–3141.

Van der Linden M, Coyette F, Poitrenaud J, Kalafat M, Calicis F, Wyns C, Adam S (2004): L'épreuve de rappel libre/rappel indicé à 16 items (RL/RI-16). L'évaluation des troubles de la mémoire: Présentation de quatre tests de mémoire épisodique avec leur étalonnage. Marseille: Solal. pp 25–47.

Watanabe S (1960): Information theoretical analysis of multivariate correlation. IBM J Res Dev 4:66–82.

Wheschler D (1981): Manual for the Wheschler Adult Intelligence Scale-Revised. New York. Psychological corporation.

Yu HJ, Christodoulou C, Bhise V, Greenblatt D, Patel Y, Serafin D, Maletic-Savatic M, Krupp LB, Wagshul ME (2012): Multiple white matter tract abnormalities underlie cognitive impairment in RRMS. Neuroimage 59:3713–3722.